Corrosion fatigue analysis of NREL's 15-MW offshore wind turbine with time-varying stress concentration factors

Journal of Physics: Conference Series **2767** (2024) 062023 doi:10.1088/1742-6596/2767/6/062023

Corrosion fatigue analysis of NREL's 15-MW offshore wind turbine with time-varying stress concentration factors

James McAuliffe, Shubham Baisthakur, Brian Broderick, and Breiffni Fitzgerald

Department of Civil, Structural and Environmental Engineering, School of Engineering, Trinity College Dublin, Ireland

E-mail: jmcaulif@tcd.ie, baisthas@tcd.ie, brian.broderick@tcd.ie, breiffni.fitzgerald@tcd.ie

Abstract. Over the last twenty years, significant development in wind turbine technologies has led to a dramatic increase in the scale of wind turbines with many now beginning to be installed in offshore locations. Consequently, modern multi-megawatt offshore wind turbines are exposed to increased cyclic loading in addition to an increased risk of corrosion attack. The combination of these two factors may result in wind turbine support structures becoming increasingly vulnerable to fatigue corrosion. The objective of this work is to investigate the impact of material thinning in fatigue-prone areas with respect to fatigue loading and ultimately to examine the potential repercussions on the lifespan of wind turbine support structures. To achieve this, a composite model is constructed coupling results from a multi-body structural dynamic model with time-varying Stress Concentration Factors (SCF) obtained from a finite element model (FEM) of NREL's 15-MW monopile-based offshore wind turbine. The nonlinear aeroelastic multi-body dynamic model of the wind turbine is used to generate stress time histories for a set of environmental conditions based on the operational conditions of the wind turbine. The finite element model of the wind turbine is then used to identify fatigue-vulnerable regions in the wind turbine support structure and calculate SCFs for these specific areas. The integration of SCFs into the fatigue calculations reduced the lifespan of the turbine tower by a factor of 4, demonstrating the importance of precisely modelling such local stress concentrations for effective fatigue analysis. A novelty of this work arises in the ability of the finite element model to update the SCFs of the fatigue-prone areas over time as corrosion-induced wastage alters the substructure's geometry, thereby inducing a global redistribution of stresses. A fatigue analysis is carried out availing of the SCFs which vary annually in addition to the stress-time histories produced by the multi-body dynamic model. The results illustrate that the phenomenon of corrosion thinning induced an 8.9% reduction in the fatigue life of the wind turbine tower, thus emphasising the significant importance of proactive maintenance strategies to mitigate the impact of corrosion.

1. Introduction

Over the last two decades in an endeavor to begin competing with conventional fossil fuels, wind turbine technology has made significant strides towards capturing greatly increased amounts of energy. In pursuit of this, wind turbines have increased dramatically in size, and in more recent times turbines are beginning to be located in offshore locations. The MySE 16-260 wind

turbine with a hub height of 152 meters and a rotor diameter exceeding 260 meters located offshore in China's Fujian Province stands as the largest wind turbine in the world. Wind turbines of similar scale to this are now being deployed globally, making today's modern multi-megawatt wind turbines the largest rotating structures in the world [1]. Offshore wind turbines must endure harsh environmental conditions, being exposed to highly fluctuating wind speeds, volatile sea states, and a corrosive marine environment. Over lifetimes in excess of 20 years, wind turbines can experience more than 10 million load cycles making them and their various components extremely susceptible to fatigue damage [2]. The IEC International Standard 61400-1 2019 [3] suggests that "Fatigue damage shall be estimated using an appropriate fatigue damage calculation", it further provides Palmgren-Miner's rule with S-N curves as an example of an appropriate fatigue damage calculation. This standard approach has therefore been adopted by a large volume of the literature available on the fatigue analysis of wind turbines [4, 5, 6, 7, 8, 9] and is further employed in this study.

As wind turbines have grown in size over the last twenty years, so too have their support structures. Wind turbine monopiles have significantly increased in both diameter and shell thickness in order to withstand the additional loads induced by their increased scale. The enlargement of wind turbines has led to greater significance of areas such as circumferential welds and connection flanges where stress concentrations can develop [10]. The failure of components such as connection flanges can cause total turbine collapse [11, 12] leading to large financial losses, thus increasing the levelised cost of energy (LCOE).

Stress Concentration Factors (SCF) can typically be calculated using empirical equations or by numerical methods such as finite element analysis. For substructures with tubular bracing several empirical approaches such as the Efthymiou empirical formula [13] are available to calculate SCFs at fatigue-critical locations such as the brace-chord intersection avoiding the requirement for finite element modelling. This paper however focuses on the fixed base monopile support structure of the IEA 15-MW wind turbine, in this support structure the transition piece is connected to the turbine tower via a bolted ring flange connection. The monopile substructure design is currently the most commonly adopted support structure for offshore wind turbines having the largest percentage of installed capacity in Europe [14]. However, literature in the area of the monopile/transition piece to tower flange connection is thus far limited despite findings in papers such as Zou et al [15] which states that the high-stress concentrations resulting from flange-to-tower connections have led to multiple failures of onshore wind turbines. The paper further highlights the issue that the existing literature surrounding fatigue damage of wind turbine towers does not consider the effect of local geometry.

In an effort to examine the significant fatigue loading that may occur in welded flange necks Seidel [16] proposed an analytical model for the calculation of SCFs under ideal conditions. The analytical approach was compared with a 3D finite element model showing good agreement. In a later paper, Seidel et al [17] investigated the impact of flange dimensions and imperfections in the flange geometry on these SCFs. It was found that connections with large shell thicknesses are increasingly likely to be critical, additionally, it was noted that geometric imperfections have negligible influence on the SCFs. Tran et al [12] carried out a convergence analysis using a finite element model of wind turbine tower flange joints with varying geometrical parameters. This parametric study enabled design modifications that reduced the maximum stresses in the flange by 22%, additionally, it concluded that the flange-to-shell junction is a critical location that can result in high stress concentrations leading to fatigue failure in L-type joints. Ji et al [18] assessed the influence of the geometrical imperfection of flatness divergence (i.e the deviation from the perfect coupling of the connection surfaces) on the fatigue life of tower shells in both floating and fixed base offshore wind turbine connection flanges. A global dynamic analysis was performed using the software package SESAM to calculate the forces and moments experienced by the ring flange. These nominal stress were then used to perform a global fatigue analysis

identifying the critical details for fatigue, following this a local fatigue analysis was performed on these details via modal superposition concepts. It was concluded that the presence of flatness divergence has a large impact, severely reducing the fatigue life of the bolted flange.

Furthermore, with modern wind turbines now being installed in offshore locations, these areas of high SCFs are additionally subjected to increased rates of corrosion. This increased risk of corrosion attack in addition to the increase in turbine scale can lead to wind turbine support structures becoming vulnerable to fatigue corrosion [19]. Okenyi et al [20] performed a stress analysis of the IEA 15-MW offshore wind turbine subjected to corrosion via Euler-Bernoulli beam theory and finite element analysis. The results of the two analyses' showed good agreement illustrating the increase in stresses observed in the turbine support structure and tower that arise due to the corrosion. The paper demonstrated the importance of considering material wastage due to corrosion in stress analysis to provide safe and accurate designs. Zhang et al [21] proposed a probabilistic Corrosion-Fatigue (C-F) deterioration model for high-strength bolts of wind turbine flange connections. This model implemented a load transfer function according to the Schmidt and Neuper approach with SCFs calculated from a detailed stress analysis with multi-physics simulations to calculate the stress ranges experienced by the turbine bolts which is applied with the C-F model. The study found that due to the effects of corrosion fatigue the lifespan of the bolt can be reduced to only 30.4% of its original expected lifespan.

The primary objective of this work is to investigate the impact of material thinning of elements in fatigue-prone areas such as connection flanges. The effects of corrosion are studied regarding fatigue loads and hence the lifespan of wind turbine support structures. In order to carry out this fatigue analysis, a composite model is implemented coupling results from a multi-body structural dynamics model with SCFs obtained from a finite element model of the wind turbine. This work is based on NREL's 15-MW monopile-based offshore wind turbine [22]. This state-of-the-art reference wind turbine features dimensions of a similar scale to the MySE 16-260 wind turbine boasting a hub height of 150 meters, a rotor diameter of 240 meters, and a steel monopile base diameter of 10 meters. The offshore location and large-scale dimensions of this wind turbine may introduce an element of vulnerability to large fatigue loads and corrosion.

2. Method

In order to create the composite model both a multi-body dynamic model and a finite element model of the wind turbine were required to be constructed and coupled. The turbine selected for this study is the IEA state-of-the-art 15-megawatt offshore reference wind turbine [22]. The key properties of this turbine can be viewed in Table 1. Once created, the composite model can be used to extract stress time histories in fatigue-prone areas. The results of the composite model can then be processed to calculate the lifetime damage experienced by the wind turbine. The details regarding the construction and validation of these models in addition to the fatigue analysis performed are presented in this section.

2.1. Multi-body Structural Dynamic Model

Time histories comprising of displacements at the top of the wind turbine tower and stresses at the base of the tower are obtained by performing numerical simulations on an aeroelastic multi-body dynamic model of the 15-MW wind turbine. The dynamic model is fully coupled incorporating both aerodynamic and hydrodynamic loading. The model which was developed using Kane's Dynamics [23] implements 22 degrees of freedom to describe the motion of the turbine components. This includes six degrees of freedom of the platform, three translational and three rotational, four degrees of freedom which describe the elastic deflections of the tower based on the first two mode shapes of the tower in both the side-to-side direction and the fore-aft direction, one degree of freedom owing to the yawing of the nacelle, one degree of freedom which describes the generator azimuth angle or rotor angle, one degree of freedom to describe

the torsional rotation of the low speed shaft, and nine degrees of freedom to describe the elastic deflections of the three blades based on the first and second flapwise mode shapes and the first edgewise mode shape.

Parameter	Value
Turbine class	IEC Class 1B
Specific rating	332W/m2
Rotor orientation	Upwind
Number of blades	3
Rotor diameter	240m
Hub height	150m
Blade length	117 m
Blade mass	65,250 kg
Root diameter	5.2 m
Max chord	5.77 m
Tip prebend	4 m
Precone	4 deg
Cut-in wind speed	3m/s
Rated wind speed	10.59m/s
Cut-out wind speed	25m/s
Design tip-speed ratio	90
Minimum rotor speed	5rpm
Maximum rotor speed	7.56rpm
Maximum tip speed	95m/s
Design tip-speed ratio	9
Drivetrain	Direct drive
Shaft tilt angle	6 deg
Rotor nacelle assembly mass	1,017t
Transition piece height	15m
Monopile embedment depth	45m
Monopile base diameter	10m
Tower mass	860t
Monopile mass	1,318t

Table 1: IEA 15-MW specification

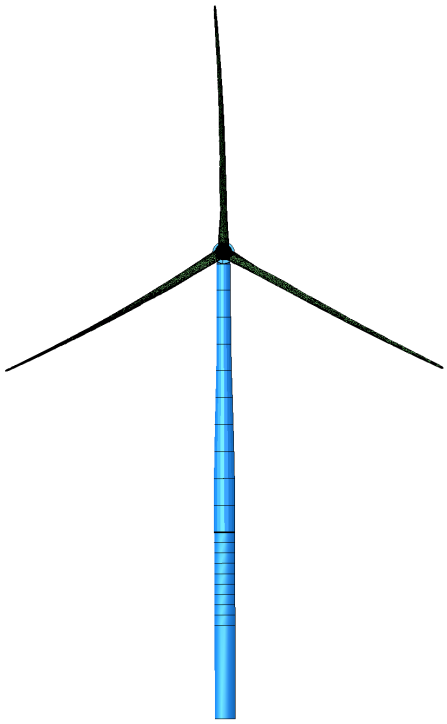

Figure 1: IEA 15-MW wind turbine FEM

The generalised equilibrium equations based on Kane's Dynamics for a simple holonomic multi-body system can be expressed as:

$$F_r + F_r^* = 0 \qquad \text{for } r = 1, 2, \ldots N \tag{1}$$

where N represents the total number of degrees of freedom of the system.

F_r, the *generalized active force* of the r^{th} degree of freedom of the system is determined for a set of n rigid bodies defined by reference frame N_i and center of mass point X_i by:

$$F_r = \sum_{i=1}^{n} \left[{}^{E}\mathbf{v}_r^{X_i} \cdot \mathbf{F}^{X_i} + {}^{E}\omega_r^{N_i} \cdot \mathbf{M}^{N_i} \right] \tag{2}$$

where $\mathbf{F}^{X_i}$ is the force vector acting on the center of mass of point X_i and $\mathbf{M}^{N_i}$ is the moment vector acting on the N_i rigid body. ${}^{E}\mathbf{v}_r^{X_i}$ and ${}^{E}\omega_r^{N_i}$ are the partial linear and partial angular velocity of the point X_i and rigid body N_i respectively associated with the r^{th} degree of freedom in the inertial (E) reference frame. The *generalized inertia force* for r^{th} degree of freedom is given as:

$$F_r^* = -\sum_{i=1}^{n} \left[{}^{E}\mathbf{v}_r^{X_i} \cdot \left(m^{N_i} {}^{E}\mathbf{a}^{X_i} \right) + {}^{E}\omega_r^{N_i} \cdot {}^{E}\dot{\mathbf{H}}^{N_i} \right] \tag{3}$$

where it is assumed that for each rigid body N_i, the inertia forces are applied at the centre of the mass point X_i. ${}^{E}\dot{\mathbf{H}}^{N_i}$ is the time derivative of the angular momentum of the rigid body N_i about its center of mass X_i in the inertial frame [23].

Using the time derivatives of the generalized coordinates of the system, the partial linear and angular velocities of significant points and rigid bodies can be established. These velocities can

then be used to write the non-linear time-domain equations of motion. These are written in their general form as:

$$\mathbf{M}(\mathbf{q}, \mathbf{u}, t)\ddot{\mathbf{q}} = -\mathbf{f}(\dot{\mathbf{q}}, \mathbf{q}, \mathbf{u}, t) \tag{4}$$

where, $\mathbf{M}$ is the inertial mass matrix that is a non-linear function of the set of degrees of freedom $\mathbf{q}$, control inputs $\mathbf{u}$, and time t. The force vector $\mathbf{f}$ depends non-linearly on the degrees of freedom, the time derivative of the degrees of freedom, control input and time. This system of equations is solved via MATLAB ® [24] employing the Runga-Kutta 4^{th} order method. For further details on the derivation of these equations, the reader can refer to Sarkar et al [25].

The wind turbine is controlled using the NREL Reference OpenSource Controller (ROSCO) [26]. The hydrodynamic loads implemented in this dynamic model are calculated using Morison's equation [27], with model constants specified as $C_M = 1.969$ and $C_D = 0.6$. The aerodynamic loads are calculated using blade-element momentum theory solved using a root finding method proposed by Ning [28]. This model has been validated using code-to-code comparison against the state-of-the-art wind turbine simulator openFAST which has been provided by NREL. The responses of the two models show good agreement, a sample of these results have been illustrated in figure 2 with further details available in Baisthakur and Fitzgerald [29].

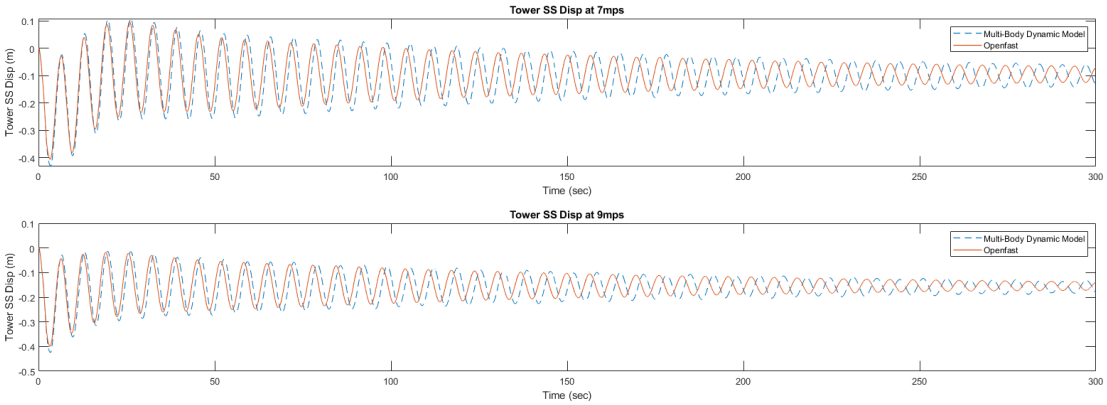

Figure 2: Multi-body dynamic model verification - comparison of tower response

This multi-body dynamic model is used to generate displacement/stress time histories for a set of environmental conditions based on the operational conditions of the wind turbine, DLC 1.2 [3]. Latin Hypercube Sampling is used to randomly select 40 wind speeds from within the cut-in to the cut-out range of the wind turbine, 3 m/s to 25 m/s respectively. The wind files for this model are generated via TurbSim [30] with a 10% turbulence intensity producing spatiotemporal turbulent velocity fields with each file being generated using a unique random seed. For this study, a location in China's Fujian province is selected, the 40 wind speeds selected for this location are assumed to be distributed via a Weibull probability distribution. Hydrological and meteorological observations presented by Yao et al [31] for this site are used with the 40 wind speeds generated to produce suitable environmental conditions at this location. Table 2 presents the range of the environmental conditions at this chosen location. The files for these sea states are generated with HydroDyn employing the Airy wave theory, assuming that the wind and wave loadings are aligned for the full duration of the simulation. In total a comprehensive suite of 240 simulations are executed each generating time histories consisting of displacements at the turbine tower top and stresses at the base of the tower. These simulations are carried out as per the recommendations in IEC 61400-1 [3] for fatigue analysis producing six 10-minute simulations for each environmental condition. For each simulation, a total time of 675 seconds is simulated with the initial 75s being removed to eliminate any initial transient effects.

Table 2: Environmental condition range

	Ws	**TI**	**Hs**	**Tp**
Min	3m/s	10%	0.62m	6.65s
Max	25m/s	10%	3.8m	8.19s

2.2. Finite Element Model

An accurate finite element model of the IEA 15-MW wind turbine is developed using Abacus software [32]. This model consists of a combination of geometric parts provided by the IEA which have been converted to be suitable for use in Abaqus in addition to parts generated from data files provided by the IEA. This model encompasses intricate components such as flanges, bearings, yaw system, and the bedplate providing a geometrically accurate representation of the turbine. Each component was assigned material properties based on those prescribed in the IEA definition of the wind turbine [22].

Due to the intricate geometry of the turbine blades and hub, the meshing software Simpleware was employed to facilitate the meshing of these components. This software implemented C3D4 elements which have high geometric versatility. The shortcomings of this element selection with regard to stiffness and mesh sizing are considered acceptable as these components are not the key focus of the study with the C3D4 element capable of capturing the mass distribution and the natural frequency of these parts [33]. All remaining parts in the nacelle of the turbine are meshed using hexahedral (brick) elements of type C3D8R, an eight-noded brick element with reduced integration preventing the effects of shear locking. In this study, the transition piece is considered to be part of the monopile as detailed by the IEA. To enable the effects of corrosion thinning to be accounted for, both the turbine tower and monopile are constructed as parametric components. Both the tower and monopile are constructed using shell elements due to their thickness dimension being significantly smaller than their other two dimensions, additionally shell elements are capable of modelling curved surfaces that undergo deformations accurately. These parts are meshed using SR4 elements, a 4-noded, quadrilateral, conventional stress/displacement shell element, in a similar manner to Hu et al [34].

The top of the monopile/transition piece is connected to the turbine tower via a flange connection designed according to the Petersen/Seidel [35] approach as per IEC 61400-6 [36]. For the purpose of this study, the only design load case from the IEC 61400-3 [37] guideline that will be considered for the ultimate load flange calculation is DLC 1.3: power production with extreme turbulence. As the remaining DLCs are neglected the load safety factor was increased from 1.35 to 2. The computed flanges have a thickness of 150mm and are connected with 180 M72 bolts of 10.9-grade high-strength steel. Further details of the flange produced can be seen in Figure 3c. The flange components are modelled as deformable parts and are coupled to the monopile and tower shell sections using a shell-to-solid coupling constraint on Abaqus. The introduction of bolts to flange connections is outside the scope of this study, to account for this adjacent flanges are connected using a tie constraint. Both flanges are meshed using a C3D20R element. The C3D20R is a quadratic brick element, with reduced integration which is a general-purpose nonlinear element. The flanges are positioned at the top of the transition piece and at the base of the tower, both the tower and monopile components are shortened by the thickness of the flange maintaining a tower top height of 144.582m. This fixed base model neglects a soil-structure interaction implementing a fixed boundary condition at the mudline of the monopile at a depth of 30m below mean sea level (MSL). The turbine is modelled in a parked condition restricting the rotation of the rotor and the pitching of the blades.

Once the construction of the finite element model was complete, a mesh convergence study was conducted on the turbine tower and monopile. This provided a suitable seed length that

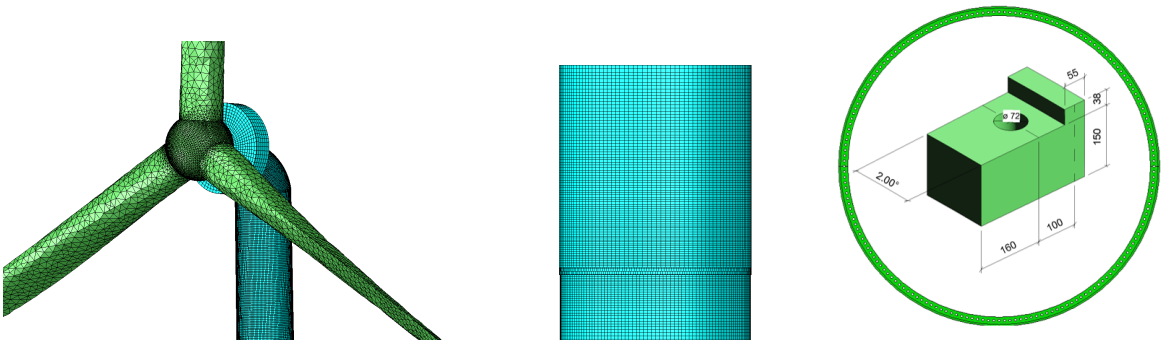

(a) Detailed mesh of hub blades and rotor (b) Tower local seeding (c) Detailed flange connection

Figure 3: 15-MW finite element model details

maximised the accuracy of the model avoiding over-stiffening arising from course meshes while reducing unnecessary simulation times. Once suitable seed lengths for both the tower and monopile were selected, in an effort to achieve increased accuracy of the analysis, local seeding was implemented in areas surrounding the connection flanges, namely the bottom sections of the tower and top sections of the monopile. The element seed length surrounding the flange connections is decreased with a single bias in the direction of the flanges as can be seen in Figure 3b. The selected seed length and local seeding implemented resulted in the finite element model being composed of over 685,000 elements.

In order to verify the accuracy of the finite element model a modal analysis was performed producing the natural frequencies and mode shapes of the structure. The first tower mode in the side-to-side direction is identified at a frequency of 0.17 hertz matching the frequency specified by NREL [22], additionally the first mode shape of the turbine tower shows good agreement with the IEA-specified mode shape from their OpenFAST software, thus verifying the model.

Following the verification of the model, a static stress analysis was carried out to identify fatigue-critical regions in the wind turbine support structure. This was performed by applying a displacement to the hub of the tower which identified the tower's shell located above the flange connection between the tower and transition piece as the location most susceptible to fatigue and hence was selected as the location to calculate the time-varying SCFs. To calculate the SCF, the maximum stress value in the shell above the connection flange is compared with the nominal stress 6.5m (mid-level of tower section) above the base of the tower where the effects of the flange connection are negligible. This stress concentration factor is then implemented with the stress values calculated using the multi-body dynamic model at a tower height of 6.5m to produce a stress time history at the tower-flange connection. A novelty of this work arises in the ability of the finite element model to implement the effective thinning of the turbine tower and flange connections once corrosion protection measures fail. The finite element model updates the SCFs of the flange tower connection annually as corrosion-induced wastage alters the substructure's geometry, thereby inducing a global redistribution of stresses. The analysis is carried out considering a number of durations for which the corrosion protection is expected to remain effective. Upon failure of corrosion protection coatings, the conventional approach of uniform corrosion is adopted. A thinning rate of 0.1 mm/year for uncoated carbon steel is applied to the substructure in the atmospheric, submerged, and buried zones while a corrosion thinning rate of 0.3mm/year is applied in the splash zone in accordance with ISO 19920 [38] and IEC 61400-1 [3]. The corrosion zones are defined in this study as per Okenyi et al [20] which implemented the DNVGL-RP-0416 guidance [39] for the IEA 15-MW wind turbine.

2.3. Fatigue Analysis

A fatigue analysis is carried out availing of the SCFs which vary annually produced by the finite element model in addition to the stress time histories produced by the nonlinear aeroelastic multi-body dynamic model. NREL's software package MLife [40] was used to calculate the accumulated fatigue damage for each year of the turbine's design life. MLife is designed based on Palmgren Miner's rule and the rainflow counting algorithm as outlined in Annex G of IEC 61400-1 [3]. A Weibull probability distribution is implemented for wind speeds coupled with their corresponding wave conditions with a shape factor of 2 and a scale factor of 10. Miner's rule is based on the concept of partial damage suggesting that damage from various periods can be summed together to calculate the total damage experienced by a component. Employing this approach with the annual fatigue damage calculated via Mlife the total fatigue damage experienced by the turbine flange connection considering the effect of corrosion thinning can be summed over a lifespan of 20 years. The results of this corrosion-fatigue analysis can then be compared with the traditional method where the support structure is assumed free from corrosion damage.

3. Results

Figure 4 displays two examples of time histories of the typical stresses experienced by the turbine tower base as calculated from the multi-body dynamic model.

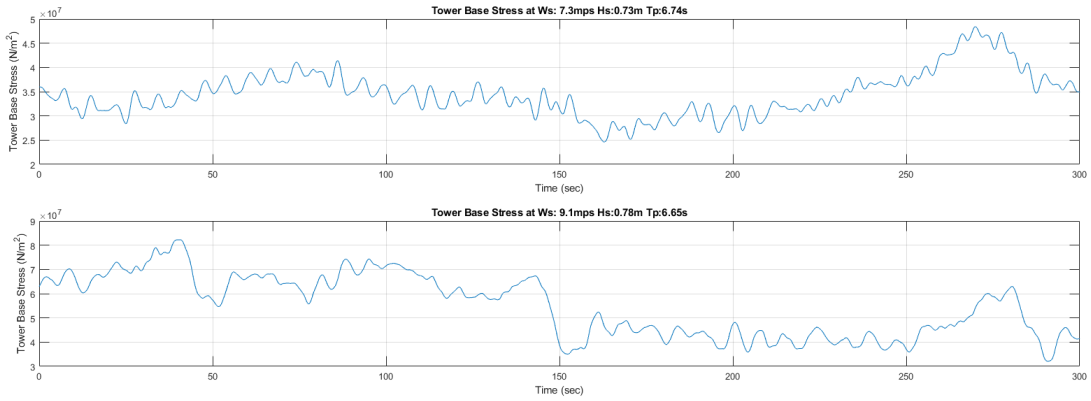

Figure 4: Tower base stress history

The phenomenon of material wastage due to corrosion has been investigated on the dominant first natural frequency of the turbine tower. A modal analysis was performed considering the corrosion protection measures to have failed after a number of durations. The percentage change in the natural frequency of the tower in the side-to-side direction is presented in Table 3 with the corrosion protection failing in increments of 5 years. The findings reveal that the natural frequency of the turbine with no corrosion protection measures applied will vary by just 2.28% over the required lifespan of 20 years. This illustrates that corrosion wastage has a negligible impact on the natural frequency of the turbine when compared with potential frequency shifts which can occur from alternative influences such as the soil-structure interaction [41].

After conducting the modal analysis, the finite element model was further employed identifying the tower shell above the flange connection between the turbine tower and the transition piece as a fatigue-critical region and hence the area on which to perform the fatigue analysis. The significance of incorporating stress concentrations stemming from the connection flange via the finite element model is evident when comparing the fatigue life with the conventional approach solely using the multi-body dynamics model. The stress concentration

Table 3: Variation in side-to-side natural frequency (%)

Corrosion protection (Years)	20	15	10	5	0
Natural Frequency shift (%)	-	-0.447	-1.02	-1.64	-2.28

results in the fatigue life reducing by a factor of 4 decreasing from a projection of 225 years to a mere 54 years. This substantial decrease in the life span of the tower component demonstrates the importance of precisely modelling such features to obtain accurate predictions.

The impact of corrosion thinning regarding the fatigue life is presented in Table 4, the analysis again explores various durations of corrosion protection. Table 4 highlights the critical importance of factoring in corrosion in fatigue estimates. Despite the turbine tower's expected fatigue life surpassing its required lifespan, by accounting for corrosion the calculated fatigue life of the wind turbine tower is decreased by almost five years curtailing the expected life span by almost 9% when no protection measures are applied. When corrosion measures are provided in wind turbines, Momber [42] suggests that many such measures, particularly in the splash zone may only survive for up to 5 years. In such instances, the results depict a significant reduction of the turbine life of over 5.5% in this case reducing the life span by over 3 years.

Table 4: Fatigue damage

Years protection	**20**	**15**	**10**	**5**	**0**
Fatigue Damage (20 Year Life)	0.370	0.373	0.379	0.391	0.406
Estimated Life Span (Years)	54.05	53.62	52.70	51.03	49.25

4. Conclusion

This work employs a sophisticated composite model integrating a multi-body dynamic model and finite element model of the IEA 15-MW offshore wind turbine. This study investigates the influence of corrosion thinning on both the natural frequency and the expected fatigue life of the wind turbine tower. The modal analysis conducted concluded that material wastage has a negligible effect on the natural frequency of the turbine tower. The finite element model identified the tower shell elements above the flange connection between the turbine tower and the transition piece as a fatigue-critical region. Consequently, a detailed fatigue analysis implementing environmental conditions based on DLC 1.2 [37] is performed, focusing particularly on this selected area of high stress.

The consideration of SCFs in the local geometry proved to be crucial for the estimations of the fatigue life of components. The SCF stemming from the flange connection reduces the fatigue life of the tower by a factor of 4 when compared with a multi-body dynamics model which neglects this feature. The effects of corrosion thinning are considered by updating the SCFs in this fatigue-prone area annually. This phenomenon is seen to have a large influence on the life span of the turbine tower reducing it by up to 8.9% emphasising the importance of including corrosion in fatigue life estimation and thus demonstrating the imperative need for regular inspection and proactive maintenance strategies to mitigate the impact of corrosion.

By implementing this approach for detailed fatigue analysis designers can derive fatigue loads with increased accuracy. This in turn will equip designers with the capability to select appropriate diameters and shell thickness of support structures thereby fostering the development of increasingly safe, sustainable and economically viable designs with the ultimate objective of reducing the levelized cost of energy production.

References

[1] Van Kuik G, Peinke J, Nijssen R, Lekou D, Mann J, Sørensen J N, Ferreira C, van Wingerden J W, Schlipf D, Gebraad P *et al.* 2016 *Wind energy science* **1** 1–39
[2] Kensche C W 2006 *International journal of fatigue* **28** 1363–1374
[3] Commission I E *et al.* 2019 *International Electrotechnical Commission, Geneva, Switzerland*
[4] Dong W, Moan T and Gao Z 2011 *Engineering Structures* **33** 2002–2014
[5] Yeter B, Garbatov Y and Guedes Soares C 2014 *Developments in Maritime Transportation and Exploitation of Sea Resources. London, UK: Taylor & Francis Group* 415–424
[6] Zwick D and Muskulus M 2016 *Wind Energy* **19** 265–278
[7] Lin M and Porté-Agel F 2020 *Journal of Physics: Conference Series* vol 1618 (IOP Publishing) p 042036
[8] Saenz-Aguirre A, Ulazia A, Ibarra-Berastegi G and Saenz J 2022 *Energy Conversion and Management* **271** 116303
[9] Wang S, Moan T and Jiang Z 2022 *Renewable Energy* **181** 870–897
[10] Yeter B, Garbatov Y and Soares C G 2015 *Engineering Structures* **101** 518–528
[11] Alonso-Martinez M, Adam J M, Alvarez-Rabanal F P and del Coz Díaz J J 2019 *Engineering Failure Analysis* **104** 932–949
[12] Tran T T, Kang S and Lee D 2022 *Energies* **15** 8967
[13] Atteya M, Mikkelsen O, Wintle J and Ersdal G 2021 *Materials* **14** 4220
[14] Redondo R and Mehmanparast A 2020 *Metals* **10** 689
[15] Zou T, Liu W, Li M and Tao L 2021 *International Conference on Offshore Mechanics and Arctic Engineering* vol 85123 (American Society of Mechanical Engineers) p V002T02A023
[16] Seidel M 2020 *Stahlbau* **89** 551–560
[17] Seidel M, Wegener F and van Dijk I 2020 *Stahlbau* **89** 932–943
[18] Ji X, Zou T, Bai X, Niu X and Tao L 2023 *Frontiers in Energy Research* **11** 1127957
[19] Li Y, Zhang Y, Wang W, Li X and Wang B 2022 *Journal of Marine Science and Engineering* **10** 1011
[20] Okenyi V, Bodaghi M, Siegkas P, Mansfield N and Afazov S 2023 *Proceedings of the Institution of Mechanical Engineers, Part C: Journal of Mechanical Engineering Science* 09544062231208551
[21] Zhang J, Heng J, Dong Y, Baniotopoulos C and Yang Q 2024 *Engineering Structures* **301** 117309
[22] Gaertner E, Rinker J, Sethuraman L, Zahle F, Anderson B, Barter G E, Abbas N J, Meng F, Bortolotti P, Skrzypinski W *et al.* 2020 Iea wind tcp task 37: definition of the iea 15-megawatt offshore reference wind turbine Tech. rep. National Renewable Energy Lab.(NREL), Golden, CO (United States)
[23] Kane T R and Levinson D A 1985 *Dynamics, theory and applications* (McGraw Hill)
[24] MATLAB 2018 *version 9.4.0 (R2018a)* (Natick, Massachusetts: The MathWorks Inc.)
[25] Sarkar S and Fitzgerald B 2021 *Energies* **14** 6635
[26] Abbas N, Zalkind D, Pao L and Wright A 2021 *Wind Energy Science Discussions* **2021** 1–33 URL `https://wes.copernicus.org/preprints/wes-2021-19/`
[27] Morison J, Johnson J W and Schaaf S A 1950 *Journal of Petroleum Technology* **2** 149–154
[28] Ning S A 2014 *Wind Energy* **17** 1327–1345
[29] Baisthakur S and Fitzgerald B 2024 *Renewable Energy* 120122
[30] Jonkman B J 2009 Turbsim user's guide: Version 1.50 Tech. rep. National Renewable Energy Lab.(NREL), Golden, CO (United States)
[31] Yao T, Lu Q, Wang Y, Zhang Y, Kuang L, Zhang Z, Zhao Y, Han Z and Shao Y 2023 *Ocean Engineering* **285** 115464
[32] Abaqus G 2011 *Dassault Systemes Simulia Corporation, Providence, RI, USA* 3
[33] Manual A U 2004 *Inc., Pawtucket, RI*
[34] Hu Y, Baniotopoulos C and Yang J 2014 *Engineering Structures* **81** 148–161
[35] Seidel M 2001 *Leibniz Universit, Hannover, Germany*
[36] IEC 2020 *International Electrotechnical Commission*
[37] 2019 *International standard IEC* 61400–3
[38] Petroleum I 2007 *International Organization for Standardization (ISO): Geneva, Switzerland*
[39] Veritas D N *Corrosion Protection for Wind Turbines*
[40] Hayman G and Buhl Jr M 2012 *National Renewable Energy Laboratory, Golden, CO* **74** 112
[41] Fitzgerald B and Basu B 2016 *Engineering Structures* **111** 131–151
[42] Momber A 2016 *Renewable Energy* **94** 314–327